Working Group 2, Deliverable 2.2

Development of PoC Demonstrators for a Number of Selected Applications

Report edited by Giulio Cossu (Scuola Superiore Sant'Anna, Pisa, Italy), Xiaodan Pang (KTH Royal Institute of Technology, Sweden) and Nobby Stevens (KU Leuven, Belgium).

June 2024

This project has received funding from the European Cooperation in Science and Technology (COST) organization under project no CA19111.

cost
European Cooperation in Science and Technology

Funded by the European Union

Contents

List of Figures

1 Introduction

This document embodies the deliverable 2 of working group 2 of the COST action project no CA19111 with the title NEWFOCUS. It consists of an ordered classification of the research efforts that have been executed by the different action participants during the final part of the project. In accordance to the project proposal, this first working group 2 deliverable is entitled “Development of PoC demonstrators for a number of selected applications”.

As one can readily observe, the efforts by the participants have been significant, demonstrating the vivid research domain of short range optical wireless communications.

2 Contributions from participants

2.1 3D Indoor Positioning with Spatial Modulation for Visible Light Communications

Researchers: **Erdal Panayirci** *1 (Kadir Has University, Istanbul,Türkiye),* **Nobby Stevens** *2 (KU Leuven, WaveCore, ESAT Ghent Technology Campus, Ghent, Belgium)*

In this work [1], a novel three-dimensional (3D) indoor visible light positioning (VLP) algorithm in Fig. 1. is proposed based on the spatial modulation (SM) and its error performance assessed as compared to the conventional received signal strength (RSS)-based 3D VLP systems [1]. As contrasted to the traditional VLP system, the proposed SM-based 3D VLP system first estimates the optical channel gain between the light-emitting diodes (LEDs) and the two photodetectors (PDs) attached to the user by a pilot-based channel estimation technique. Then, unknown 3D positions of the receiver are determined by the trilateration algorithm with distances computed from the estimates of the channel gains. Consequently, the 3D VLP system achieves an interference free transmission with increased spectral efficiency and without the need for a demultiplexing process at the receiving end. The implementation of SM not only ensures a more accurate 3D positioning by refining distance measurements through pilot-aided channel estimation but also addresses the challenges of transmission data rate constraints, all while significantly reducing positioning errors in challenging indoor environments as validated by comprehensive computer simulations. The computer simulation results show that the positioning errors are obtained in an order of magnitude smaller than RSS-based techniques in an indoor industrial environment (Fig. 2). This is mainly because the distances involved in determining the 3D positions can be determined more precisely by the pilot-aided channel estimation method without creating any data rate problem in transmission due to the higher spectral efficiency of the SM.

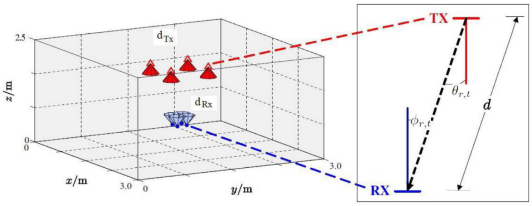

Figure 1: Indoor joint communications and VLC positioning

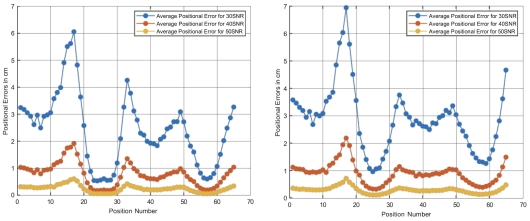

Figure 2: Average positional error curves at the 30 SNR, 40 SNR, and 50 SNR conditions: (a) z constant (two-dimensional case), (b) z variable (three-dimensional case).

2.2 Physical layer security with DCO-OFDM-based VLC under the effects of clipping noise and imperfect CSI

Researchers: *Erdal Panayici 1 (Kadir Has University, Istanbul,Türkiye), Panos Diamantoulakis 2 (University of Macedonia, Thessaloniki, Greece)*

In this work, we consider a DC-biased optical OFDM (DCO-OFDM) equipped with physical layer security (PLS) as applied to indoor VLC systems, as shown in Fig. 3 [2]. First, a novel PLS algorithm is designed to protect the DCO-OFDM transmission of the legitimate user from an eavesdropper. A closed-form expression for the achievable secrecy rate is derived and compared with the conventional DCO-OFDM without security. To analyze the security performance of the PLS algorithm under the effects of the residual clipping noise and the channel estimation errors, a closed-form expression is derived for a Bayesian estimator of the clipping noise-induced naturally at the DCO-OFDM systems after estimating the optical channel impulse response (CIR) by a pilot-aided sparse channel estimation algorithm with the compressed sensing approach. Finally, from the numerical and computer simulations, the BER performance of the proposed algorithm is compared to the one based on iterative clipping mitigation for BPSK, QPSK, and 16QAM signaling for different levels of clipping noise as $B = 0.5$, 1, and

2 dB. As shown in Fig. 4, it is concluded that the proposed algorithm contributes substantially to the BER performances of the system at every clipping noise level chosen compared to the iterative clipping mitigation-based algorithm and hence significantly reduces the nonlinear disturbance effects caused by clipping noise. It is also shown that the proposed PLS algorithm with secret key exchange guarantees the eavesdropper's BER to stay close to 0.5 and that the proposed encryption-based PLS algorithm does not affect the BER performance of the legitimate user in the system.

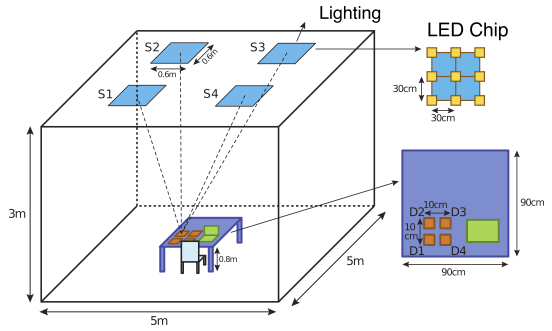

Figure 3: VLC channel model simulation environment

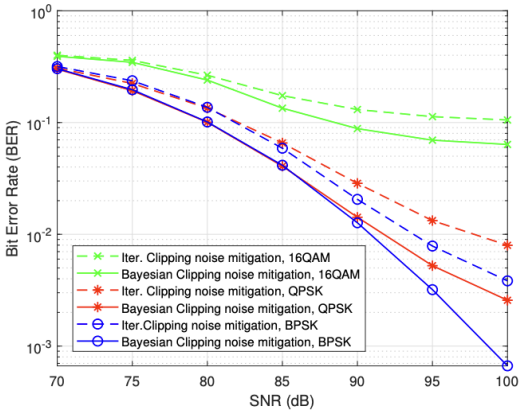

Figure 4: BER vs. SNR performances for BPSK, QPSK, 16-QAM and comparison with iterative mitigation algorithm.

2.3 Channel Estimation and Physical Layer Security in Optical MIMO-OFDM-based LED Index Modulation

Researchers: **Erdal Panayici** *1 (Kadir Has University, Istanbul,Türkiye),* **M. Ali Khalighi** *2 (Institut Fresnel Aix-Marseille University Marseille, France)*

In this work, we propose a new and low-complexity channel estimation algorithm for the generalized LED index modulation (GLIM), recently proposed for visible-light communication systems based on multi-input multi-output (MIMO) and orthogonal frequency-division multiplexing (OFDM) denoted by GLIM-OFDM. We investigate the bit-error rate (BER), the mean-square error (MSE) of channel estimation, as well as the Cramer-Rao bound on the latter. Furthermore, we present a novel physical layer security (PLS) technique for the GLIM-OFDM scheme using precoding at the transmitter, assuming it has the channel state information (CSI) between the LEDs and a legitimate user but no knowledge of the CSI corresponding to eavesdroppers. The simulation results for the PLS performance of the proposed GLIM OFDM indoor LiFi system we obtained considering three different user scenarios, as shown in Fig. 5. The symbols S1, S2, S3, and S4 represent the LEDs transmitting the four components of the OFDM complex-valued time samples. The white and black figures of the bottom one represent Bob and Eve, respectively. These scenarios are different based on the relative positions as compared to the room's middle line (dashed line). Through computer simulations based on the channel matrices of the legitimate user (Bob) and eavesdropper (Eve) acquired by Zemax© software, the BER performance of Bob and Eve is examined. As seen in Fig. 6, Bob's BER performance outperforms the performance of Eve substantially. While the BER of Bob reaches 10^{-5} at SNR values between $20 - 30$ dB, Eve's BER is not below 3×10^{-1} in a similar SNR range.

2.4 Spatial Modulation Aided Physical Layer Security for NOMA-VLC Systems

Researchers: *Erdal Panayici 1 (Kadir Has University, Istanbul,Türkiye), Harald Haas 2 (The University of Strathclyde, Glasgow, U.K.)*

In this work, we consider the physical layer security (PLS) problem in multi-user non-orthogonal multiple access (NOMA) enabled multiple-input multiple-output (MIMO) visible light communication sys-

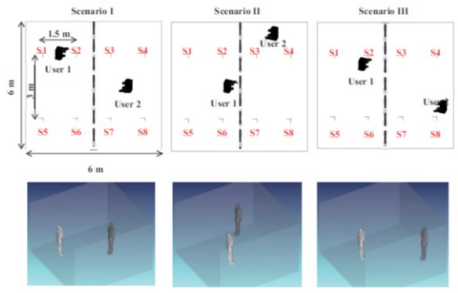

Figure 5: Locations of Bob and Eve in three different scenarios

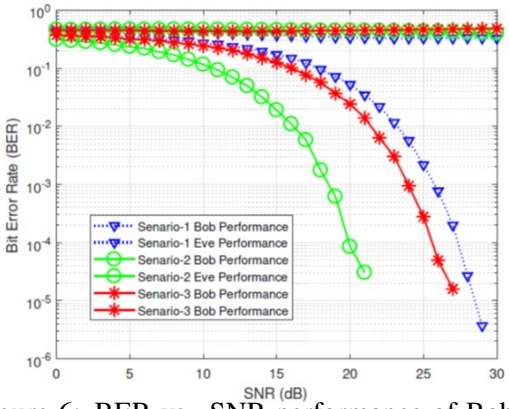

Figure 6: BER vs. SNR performance of Bob and Eve

tems intercepted by a passive eavesdropper (Eve) as shown in Fig. 7 [3]. We propose a novel transmit precoding scheme based on receive spatial modulation (RSM) to degrade the signal-to-interference-noise ratio (SINR) of Eve by exploiting only the slow-fading characteristics of the visible light channel of the legitimate users (Bobs). The proposed PLS precoder is reinforced with secret parameter exchange with Bobs, and a CSI acquisition model is proposed to reduce the PLS algorithm's computational load substantially at the transmitter. The closed-form expressions for the achievable secrecy rates and their upper and lower bounds are derived. Via Monte Carlo simulations, we confirm that Bobs can successfully decode their information in various user configurations. At the same time, Eve's received SINR is significantly worsened by the jamming signal induced by the proposed precoder with secret key exchange. It is also shown that Eve's bit error rate (BER) is increased to the 0.5 level for almost any position in the considered indoor environment. Finally, in Fig. 8, we compare the achievable secrecy capacities and the secrecy sum-capacities of the proposed PLS technique in NOMA-VLC with conventional time-division multiplexing (TDM)-based OMA-VLC benchmark scheme in the same two-user and one eavesdropper scenario. It consists of $N_t = 8, N_r = 4$ transmitting and receiving units, respectively. M-ary PAM signaling is employed with $M = 8$. Hence, the maximum information capacity between the source and each user is $\log 2(Nr) + \log 2(M) = 5$ bps/Hz. User 1 and User 2 positions are selected in the indoor test environment as $[0, 0, 0.85]$ and $[1, -3.2, 85.5]$ so that User 1 represents a strong and User 2 as a weak user according to their channel gains.

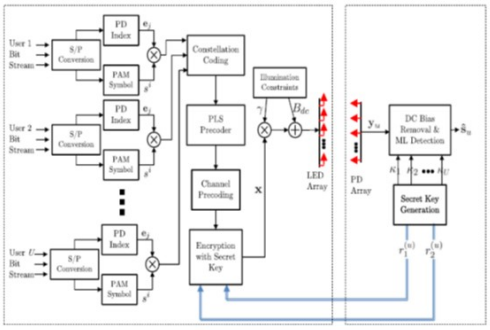

Figure 7: Proposed RSM-based PLS precoding system with secret key exchange for the multi-user NOMA-VLC.

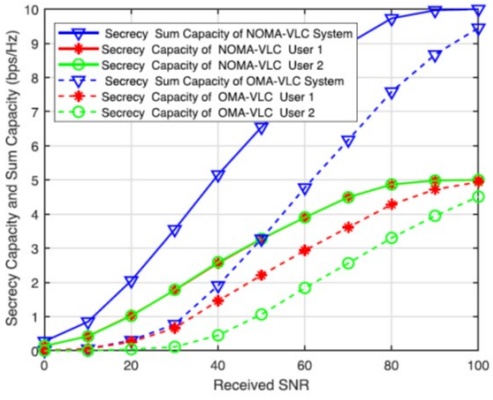

Figure 8: Comparison of the proposed NOMA-VLC system with OMA-VLC on achievable secrecy capacities.

2.5 Implementation of a High Measurement Rate VLP System

Researchers: *David Moltó (UAH, Spain), Elena Aparicio-Esteve (UAH, Spain), Álvaro Hernández (UAH, Spain), Jesús Ureña (UAH, Spain), José M. Villadangos (UAH, Spain), Miguel Cubero (UAH, Spain)*

This work presents a System-on-Chip (SoC) architecture for the real-time implementation of the signal processing algorithms for an optical indoor positioning system. It is configured using some LED beacons placed at known positions and the corresponding receivers to be positioned moving in the coverage area. The definition and design of the hardware architecture for the processing associated to the receiver, for the case of a Quadrant Photodiode Angular Diversity Aperture (QADA) detector, is proposed, analyzing different aspects involved in the final performance, such as the fixed-point notation used in the hardware definition. Furthermore, the implementation of the proposal includes an analog conditioning stage, an acquisition system, as well as a FPGA-based (Field-Programmable Gate Array) System-on-Chip (SoC) for implementing the necessary hardware and software elements, required to estimate the final position coordinates of the QADA receiver.

The definition and design of the specific peripheral, that is integrated in the SoC architecture, is proposed, analyzing the effect of the corresponding fixed-point notation. The incoming signals from the QADA can be acquired at rates up to several MHz, thus allowing the implementation of encoding techniques with LS sequences in the LEDs' transmissions. The acquired signals go through the different processing stages, where Fig. 9 shows the global block diagram of the architecture including the different peripherals designed for the processing of the signals coming from the QADA receiver. The resulting ratios P_x, P_y provide information about how the upper and the bottom halves of the QADA are enlightened (P_x) or the right and left halves (P_y). These ratios are then sent to a FIFO memory block, where they will be stored until they are read by the processor. Based on them, the processor available in the proposed architecture computes the corresponding positioning algorithm to estimate the final position of the QADA receiver.

To validate the design, comparisons with test patterns have been performed for every peripheral, where 20 emissions are captured and processed in the proposed architecture to obtain the final ratios Px and Py using the experimental setup detailed in Fig. 10 a). The values resulting from the hardware architecture are compared with those obtained in Matlab© as shown in Fig. 10 b). It is possible to highlight that, in the demodulation, correlation, and maximum detection stages, quantization errors are null, whereas, when obtaining the ratios P_x and P_y, the absolute errors are 0.00018 and 0.00002, respectively. In addition, two test points have been considered here: no. 1 located under the beacon B2, and no. 2 in the middle of the square formed by the beacons. The mean estimated errors for coordinates x, y and z are 0.4cm, 0.6cm, 1.3cm, and 1.5cm, 3.2cm, 4.4cm for point no. 1 and no. 2, respectively, whereas the standard deviations of errors remain below 20 cm in the worst case.

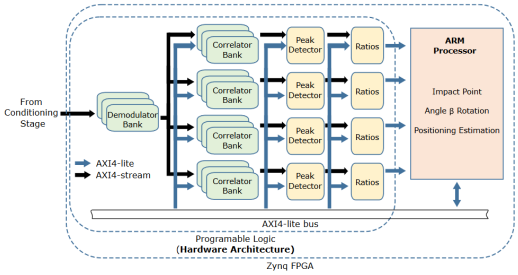

Figure 9: General block diagram of the proposed SoC architecture, consisting of the different peripherals involved in the signal processing of the signals coming from the QADA sensor.

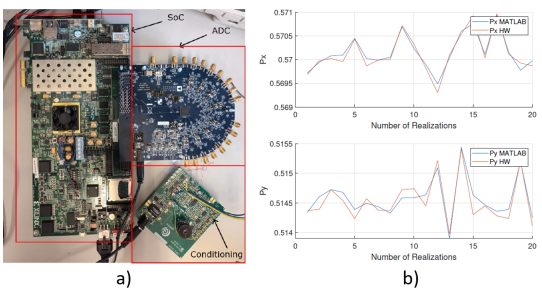

Figure 10: Experimental evaluation of the proposal: a) Experimental setup ; b) Estimates of the ratios P_x and P_y.

Funded by the European Union

2.6 Experimental Demonstration of Integrated Optical Wireless Sensing and Communication

Researchers: *Lina Shi (LISV-UVSQ, France), Ziqi Liu (LISV-UVSQ, France), Bastien Béchadergue (LISV-UVSQ, France), Hongyu Guan (LISV-UVSQ, France), Luc Chassagne (LISV-UVSQ, France) and Xun Zhang (ISEP and LISV-UVSQ, France*

While the contours of 6G are still being defined, integrated sensing and communication (ISAC) has been identified by the International Telecommunications Union (ITU) as a key feature of next-generation wireless communications. Given the maturity already demonstrated for data transmission on the one hand, and positioning on the other hand, optical wireless communications (OWC) could offer promising solutions for ISAC implementation, especially in indoor scenarios. In this paper, we propose and implement an OWC-based ISAC system that relies on multi-band carrierless amplitude and phase (m-CAP) modulation associated with received signal strength (RSS)-based positioning to achieve data transmission and localization from the same signal. This m-CAP/RSS system is deployed in a $1.2\times1.2\times2.16$ m room using four access points (AP) installed on the ceiling, and can provide a communication link at a data rate of 12 Mbps with a bit error rate of less than 3.8×10^{-3} to any user equipment (UE) in a reception plane 20 cm above the ground, while estimating its position with an error of less than 5.9 cm in 90% of cases.

The implemented demonstrator mainly relies on an Ettus USRP X300 platform coupled with custom-made optical antennas and interfaced with GNU Radio and MATLAB. As visible in Fig. 11, a computer ① is used to first generate the m-CAP signal with MATLAB, and then transmit it to the USRP X300 ② via an Ethernet link controlled by the GNU Radio software. The USRP then transmits in loop the m-CAP waveform in its baseband analog form thanks to an Ettus BasicTX daughterboard. However, this analog signal has a too low peak-to-peak amplitude to drive the AP's optical antenna correctly, and must therefore be amplified beforehand. A Mini-Circuit ZHL-6A-S+ power amplifier ③, coupled to two 6 dB SMA attenuators, and powered by an external power supply ④, is therefore added at the output of the USRP X300.

As shown in Fig. 12, this optical antenna ⑤ is installed on the ceiling of a $1.2 \times 1.2 \times 2.16$ m test area. At the other end of the link, a second optical antenna ⑥, this time serving as a UE, is mounted on a double rail ⑦ enabling it to be positioned precisely in an x-y receiving plane, located at a distance $h' = 20$ cm from the ground, so that the vertical distance between AP and UE is $h = 1.96$ m. The entire test area is protected from external light interference by black curtains ⑧. The UE's optical antenna, fed on the one hand by the external power supply ④, is on the other hand connected to the USRP X300 ②, which uses a BasicRX daughter board to convert the received analog signal into its digital equivalent. This digital signal is eventually recorded as a vector of samples, and post-processed with MATLAB on the computer ① in order to evaluate the communication and positioning performance of the proposed system. The whole procedure was then repeated after placing the AP's optical antennas at four successive and different position so that the RSS positioning technique can then be applied.

Figure 13 shows the positioning results obtained, with in blue circle the reference positions of the UE, in red crosses the estimated positions before correction and in black crosses the estimated position after correction (a two-step process not detailed here but which consists in estimating the direction of the error and removing the average error over the whole plane along this direction). The estimated positions corresponding to a given reference position are in addition linked to the latter by a grey dashed line to ease the understanding of the results. When plotting the cumulative distribution function of the positioning errors obtained after correction, it appears that 90% of these errors remain below 5.9 cm. At the same time, exploitation of the communication data show that the BER remains below $3.8\times10-3$ over the whole reception with an outage probability of 0.7%.

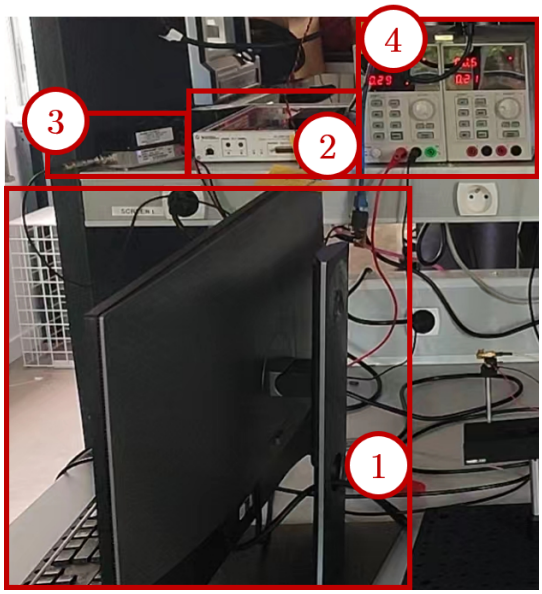

Figure 11: Control area of the ISAC prototype, with ① the control computer for signal modulation and post-processing, ② the USRP X300, ③ a power amplifier for transmit signal amplification and ④ the power supply.

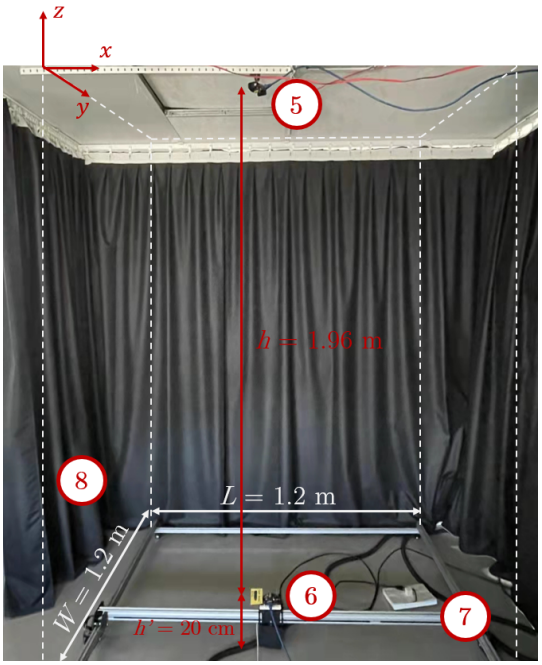

Figure 12: Test area of the ISAC prototype, with ⑤ the transmit optical antenna, ⑥ the receive optical antenna, ⑦ a double rail to position the receive optical antenna and ⑧ black curtains delimiting the test area.

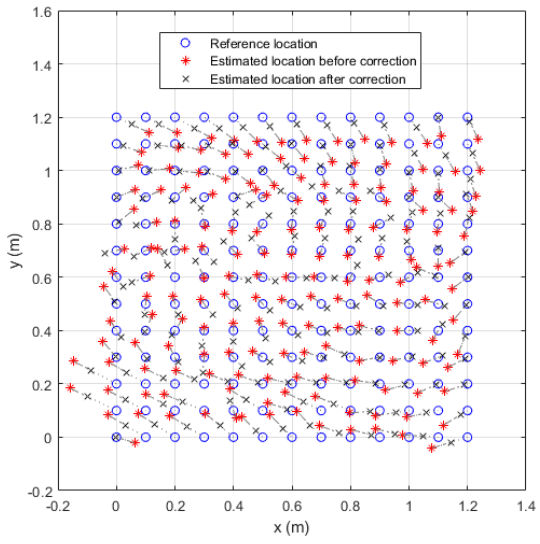

Figure 13: Top view of the reception plane with the reference coordinates and estimated coordinates before and after correction.

2.7 Audio Signal Quality Assessment in Visible Light Communication

Researchers: *Jovan Galić (University of Banja Luka, Faculty of Electrical Engineering, Bosnia and Herzegovina), Milan Mlađen (University of Banja Luka, Faculty of Electrical Engineering, Bosnia and Herzegovina), Gordana Gardašević (University of Banja Luka, Faculty of Electrical Engineering, Bosnia and Herzegovina), Milica Petković (University of Novi Sad, Faculty of Technical Sciences, Serbia), Boris Malčić (University of Banja Luka, Faculty of Electrical Engineering, Bosnia and Herzegovina), Slavko Šajić (University of Banja Luka, Faculty of Electrical Engineering, Bosnia and Herzegovina)*

Visible Light Communication (VLC) has been considered a supplementary technology to conventional Radio Frequency (RF) communication systems, offering a multitude of advantages. Several research studies have demonstrated the feasibility of employing VLC technology for reliable audio communication. The primary objective of this study is to examine the quality of the analog audio signal through the utilization of intensity modulation and direct detection (IM/DD) scheme. The low-cost transceiver based on OpenVLC1.3 RevA capes has been exploited to perform a preliminary study and evaluate the performance of an analog short-range IM/DD VLC system. The experimental testbed is depicted in Fig. 14. The main advantages of the experimental testbed are that the system exhibits low complexity and cost and that the utilization of IM/DD yields simplicity and eliminates the need to account for the phase or frequency of the receiver signal, thus establishing a non-coherent transmission. Nonetheless, a constraint in the testbed's design is its susceptibility to changes in the receiver's position and orientation, which directly affects the obtained results. The evaluation of audio quality is conducted based on the following parameters: Total Harmonic Distortion (THD), Intermodulation Distortion (IMD), Signal-to-Noise Ratio (SNR), and Signal-to-Noise and Distortion (SINAD). Furthermore, the impact of daylight illuminance levels on the mentioned parameters has also been analyzed, considering three distinct values of amplitude and bias voltage. The obtained results indicate that VLC can facilitate the transmission of audio signals with satisfactory and faithful quality, with an achieved THD level below 1

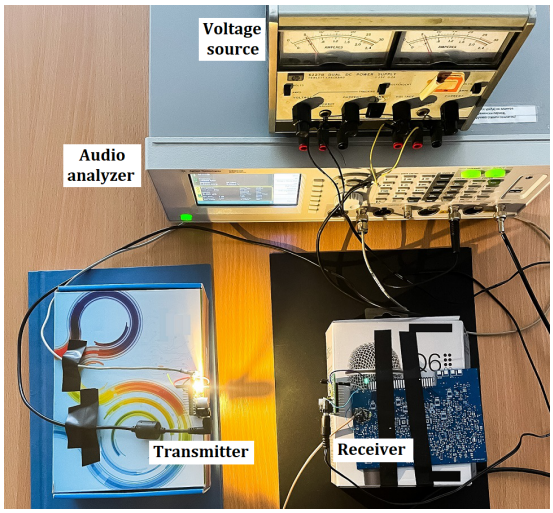

Figure 14: The experimental testbed.

2.8 Experimental Demonstration of High-Precision 3D/2D Indoor Visible Light Positioning using an Imaging Receiver

Researchers: *J. A Apolo (Universitat Politècnica de València, Spain), I. N. O. Osahon(Bangor University, U.K), B. Ortega (Universitat Politècnica de València, Spain), V. Almenar (Universitat Politècnica de València, Spain), J. Tang(Bangor University, U.K), S. Rajbhandari (University of Strathclyde, U.K)*

This work proposes a novel highly accurate 2D/3D VLP approach using a 2D array of diversity receivers in conjunction with a supervised artificial neural network (ANN). The ANN is trained to estimate po-

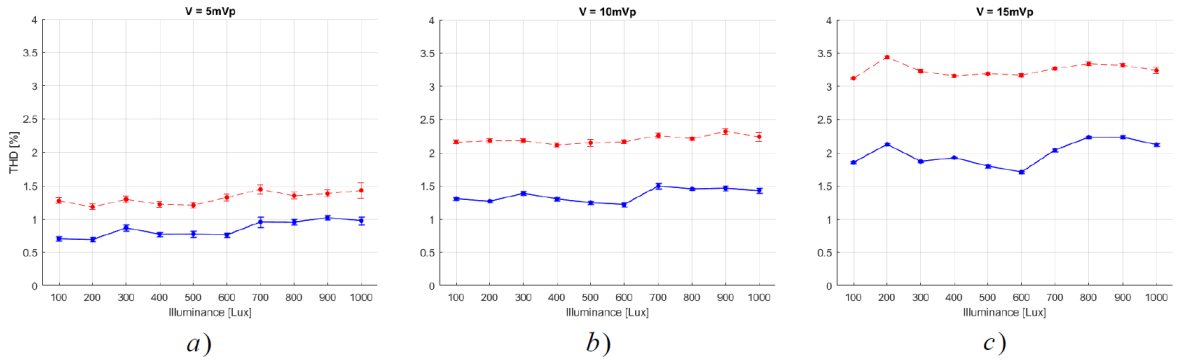

Figure 15: The THD parameter results (offset voltage 2.26V dashed; 2.30V solid).

sitions based on the received signal strength (RSS) from various transmitters (Tx) to multiple receivers (Rx). In our proof-of-concept demonstration, we deployed four ceiling-mounted illumination sources as transmitters and positioned an imaging receiver 1.4 m away. The experimental results show position accuracies of 4 mm and 55 mm for 2D and 3D positioning, respectively.

Fig. 16 shows the laboratory setup of the positioning system with the proposed image receiver. For 2D/3D positioning estimation, a supervised fully-connected feed-forward back propagation multi-layer perceptron (MLP) ANN with one input layer, one hidden layer and one output layer is implemented. The number of neurons in the input layer equals NTx $\times$ NRx corresponding to RSS matrix for a particular position. The output layer has two or three neurons corresponding to the estimated position coordinates for 2D or 3D positioning, respectively. The hidden layer is 32 neurons with a sigmoid transfer function.

To assess 2D positioning, we captured a total of 784 points within a 41×41 cm^2 area. For 3D positioning, we used a total of 1880 points within a $54 \times 51 \times 12$ cm^3 volume. In both cases, 90 % of the RSS values were used to train the system, while the remaining 10 % was used to test the positioning accuracy. The preliminary evaluation has demonstrated a geometric error of 4 mm for the 2D positioning scenario and an accuracy of 58 mm for the 3D positioning scenario at 0.9 CDF.

The system performance evaluation also examined the effect of receiver diversity for 2D and 3D positioning, as shown in Fig. 17 (a) and (b), respectively. The criteria adopted to evaluate the results is the cumulative distributive function (CDF) of the positioning error across the room. The results demonstrate the impact of receiver diversity on system accuracy. In the case of 2D positioning, the positioning error for 0.9 CDF decreases from 30 mm when using a single PD, to 6 mm when using two PDs, to 5 mm when using three PDs and reaches 3.7 when using all four PDs. For 3D positioning, an error of 78 mm is recorded with a single PD, 60 mm with two or three PDs and 55 mm with all four PDs active.

This work presents an experimental implementation of a highly accurate visible light positioning system using receiver diversity. The approach is based on the measurement of the RSS and the use of ANN. An experimental evaluation of the performance of an imaging system consisting of one lens and four photodetectors was conducted to introduce diversity in the receiver. The future work includes the optimization of VLP by incorporating optical simulations with the experimental set-up.

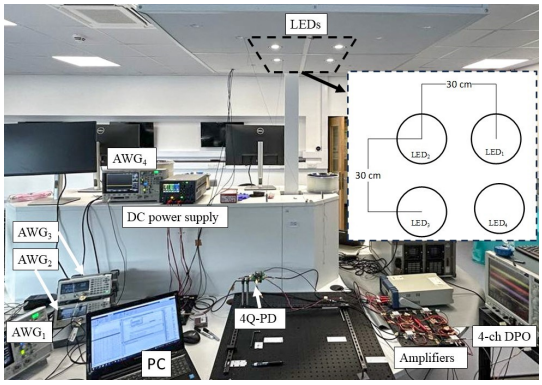

Figure 16: VLP lab experimental setup. The inset shows the geometrical distribution of the transmitters.

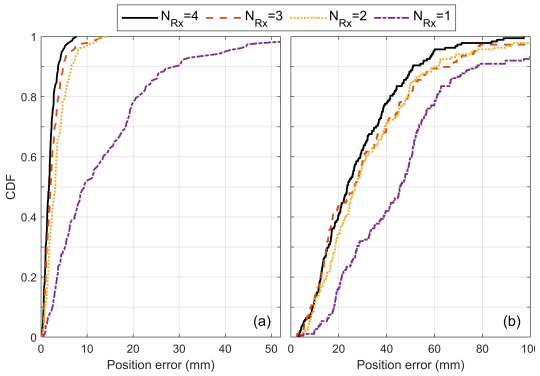

Figure 17: CDF of geometrical error of a four-luminaire system using different number of PDs for comparative evaluation.

References

[1] Umit Sen, Yalin Evrim Yesilirmak, Irem Ozgur Bayman, Taner Arsan, Erdal Panayirci, and Nobby Stevens. 3d indoor positioning with spatial modulation for visible light communications. *Optics Communications*, 529:129091, 2023.

[2] Erdal Panayirci, Ekin Bektaş, and H. Vincent Poor. Physical layer security with dco-ofdm-based vlc under the effects of clipping noise and imperfect csi. *IEEE Transactions on Communications*, PP:1–1, 01 2024.

[3] Erdal Panayirci, Mutlu Koca, Harald Haas, and H. Vincent Poor. Spatial modulation aided physical layer security for noma-vlc systems. *IEEE Transactions on Vehicular Technology*, PP:1–16, 08 2023.